Sedimentary Geology 316 (2015) 1–12

Contents lists available at ScienceDirect

Sedimentary Geology

journal homepage: www.elsevier.com/locate/sedgeo

Provenance of sands from the confluence of the Amazon and Madeira rivers based on detrital heavy minerals and luminescence of quartz and feldspar

Daniel R. do Nascimento Jr. [a,b,*], André O. Sawakuchi [a], Carlos C.F. Guedes [c], Paulo C.F. Giannini [a], Carlos H. Grohmann [d], Manuela P. Ferreira [a]

[a] Instituto de Geociências, Universidade de São Paulo, Rua do Lago 562, São Paulo, SP 05508-080, Brazil
[b] Departamento de Geologia, Universidade Federal do Ceará, Campus do Pici, Bloco 912, Fortaleza, CE 60455-760, Brazil
[c] Departamento de Ciências do Mar, Universidade Federal de São Paulo, Av. Alm. Saldanha da Gama 89, Santos, SP 11030-400, Brazil
[d] Instituto de Energia e Ambiente, Universidade de São Paulo, Av. Prof. Luciano Gualberto 1289, São Paulo, SP 05508-010, Brazil

ARTICLE INFO

Article history:
Received 6 September 2014
Received in revised form 17 November 2014
Accepted 18 November 2014
Available online 27 November 2014

Editor: J. Knight

Keywords:
Provenance
Amazonian rivers
Heavy minerals
Optically stimulated luminescence

ABSTRACT

Source-to-sink systems are poorly known in tropical rivers. For the Amazonian rivers, the majority of the provenance studies remain focused on the suspended load, implying a poor understanding of the processes governing production and distribution of sands. In this study, we perform heavy mineral and optically stimulated luminescence (OSL) analysis to cover the entire spectrum (heavy and light minerals fraction) of 29 sand samples of the Lower Madeira river region (Amazon and Madeira rivers), of which the main goal was to find provenance indicators specific to these rivers. Despite the tropical humid climate, the sands of the Amazon and Lower Madeira rivers are rich in unstable heavy minerals as augite, hypersthene, green hornblende and andalusite. The Madeira river is highlighted by its higher content of andalusite, with source attributed to the Amazon Craton (medium-to-high grade metamorphic rocks), while the Amazon river, upstream of the Madeira river mouth, has a signature of augite and hypersthene, that suggests an Andean provenance (volcanic rocks). Sands from the Madeira river can be tracked in the Amazon river by the increasing concentration in andalusite. OSL analysis of the light minerals fraction was used as an index of feldspar concentration and sedimentary history of quartz grains. Lower feldspar concentration and quartz grains with longer sedimentary history (higher OSL sensitivity) also point to a major contribution of cratonic sources for the sands in the Madeira river. While the sands from the Lower Madeira would be mainly supplied by cratonic rocks, previous work recognised that suspended sediments (silt and clay) are derived from Andean rocks. Therefore, we interpret a decoupling between the sources of sand and mud (silt and clay) under transport in the Madeira river. Andean sands (rich in augite and hypersthene) would be trapped in the foreland zones of the Beni and Mamoré tributaries. In the Amazon river sands, the low OSL sensitivity of the quartz, higher content of feldspar and unstable heavy mineral assemblage dominated by augite and hypersthene suggest both a fast transport from Andean sources with fine sediment bypass over foreland areas.

1. Introduction

There is great debate about the evolution of the Amazonian river system, especially with regard to its onset to a transcontinental west to east drainage (Campbell et al., 2006; Figueiredo et al., 2009; Shephard et al., 2010; Sacek, 2014). Provenance questions are in the core of this debate because Andean sediments reaching the present Amazon river mouth could be the fingerprint for the development of a transcontinental river. Using sediment characteristics to deduce changes in a river system requires the understanding of factors controlling the production (source), transport and accumulation (sink) of sediments. Under this approach, sediments and sedimentary rocks are products of a source-to-sink system (Allen and Allen, 2005) operating on different temporal and spatial scales. Determining sediment provenance and reworking (i.e., number of burial-erosion cycles during sediment transport) can be considered two fundamental tasks to describe the Amazonian river system under a source-to-sink perspective (Blatt, 1967; Pettijohn et al., 1972; Pettijohn, 1975; Everett and Rye, 2003; Allen, 2008; Carter et al., 2010; Marsaglia et al., 2010; Wolinsky et al., 2010).

* Corresponding author at: Departamento de Geologia, Universidade Federal do Ceará, Campus do Pici, Bloco 912, Fortaleza, CE 60455-760, Brazil. Tel.: +55 85 33669867; fax: +55 85 33669874.
E-mail addresses: danieljr@usp.br, daniel.rodrigues@ufc.br (D.R. do Nascimento), andreos@usp.br (A.O. Sawakuchi), ccfguedes@gmail.com (C.C.F. Guedes), pcgianni@usp.br (P.C.F. Giannini), guano@usp.br (C.H. Grohmann), manu_pf7@yahoo.com.br (M.P. Ferreira).

http://dx.doi.org/10.1016/j.sedgeo.2014.11.002
0037-0738/

Sediment provenance and reworking are mutually related and are essential to define proxies able to record spatial and temporal variations in production, transport and deposition of sediments.

Large rivers from tropical settings such as the Amazon are part of the major active source-to-sink systems around the world. The Amazon watershed and its subaqueous fan represent the biggest active source-to-sink system in terms of sediment load in South America (Latrubesse et al., 2005). The Amazon river accounts for more than 70% of the sediment load reaching the South Atlantic ocean (Meade et al., 1985). In this context, the Madeira river stands out as one of the major tributaries of the Amazon river, from which approximately 2.76×10^9 tonnes/year of suspended sedimentary load is delivered to the Amazon river (Meade et al., 1985; ANA, 2014). The Madeira river drains terrains with distinct elevation, climate, vegetation cover and land use and it supplies around 15% of the Amazon river waters (Latrubesse et al., 2005). Factors such as catchment size and intense channel migration dynamics (i.e., meandering, avulsion) make large rivers subjected to complex changes in sediment sources, storage and reworking through time (i.e., Stouthamer and Berendsen, 2001; Slingerland and Smith, 2004). Temporary sediment storage in stabilised bars and floodplains can promote mixing of sediments from different sources and produced under distinct climate or tectonic conditions. Sedimentary reworking within the fluvial system can occur, for example, by means of erosion of ancient bars and abandoned meanders. In large rivers, the control in sediment mixing and reworking goes beyond the action of autocyclic phenomena of meandering or channel avulsion. Allocyclic factors, such as tectonics and climate changes, are also important, especially on millennial timespans (Stouthamer and Berendsen, 2007). Therefore, the study of sediment provenance, mixing and reworking in large tropical rivers is necessary to understand how sediment properties may record allocyclic changes. This is still poorly understood for Amazonian rivers, especially with regard to the sand supply. Most previous studies of the Amazonian rivers focus on the suspended load using geochemical approaches (Martinelli et al., 1993; Meade, 1994; Filizola, 1999; Bouchez et al., 2011; Govin et al., 2014). This paper investigates provenance and sedimentary reworking of sands of the Madeira river supplied to the Amazon river. For this, we performed heavy mineral analysis (Morton and Hallsworth, 1994, 1999) combined with optically stimulated luminescence (OSL) sensitivity (Pietsch et al., 2008; Sawakuchi et al., 2011, 2012) for provenance and sediment reworking analysis of sand from bars and the bottom channel in the confluence of the Madeira and Amazon rivers.

2. Physiography, geology and fluvial hydrology of the Amazon and Madeira rivers

The Amazon river, in its portion upstream of the Madeira river mouth, is formed by the coalescence of numerous drainages sourced in the Andean region of Peru, Ecuador and Colombia and flowing to the Amazonian plains (mainly in Brazil) (Meade et al., 1985), covering an area of about 3 million km^2 (Fig. 1). In turn, the Madeira river has a drainage area of nearly 1.4 million km^2, being one of the major tributaries of the Amazon river (Latrubesse et al., 2005). The upstream waters of the Madeira river are located in the Bolivian Andes, and it is formed by the coalescence between Beni and Mamoré rivers on the Bolivia-Brazil border (Hoorn, 1994; Hoorn et al., 1995).

The Amazon and Madeira rivers' watersheds present a wide variation of climatic and geomorphologic features. The climate varies from semi-arid (as in the La Paz river, mean precipitation of 200 mm/year) to hyper-humid tropical (as in the Yungas valleys, mean precipitation of 6000 mm/year) and common tropical (mainly in the Amazonian plains, precipitation of 1700–2000 mm/year) (Guyot et al., 1999; Latrubesse et al., 2005; Silva et al., 2011). The general altitudes vary from 120 to 6500 m (altitudes of the catchment areas of the Madeira river ranges 3000–4000 m; Guyot et al., 1999), locally exerting strong influence in the heavy orographic rains at the foot of the Andean Cordillera (Latrubesse et al., 2005). The precipitation is heavily seasonal, with dry and wet seasons controlled by the migration of the Intertropical Convergence Zone (ITCZ) (Vera et al., 2006; Grimm, 2011). The rainy season starts at the ITCZ moves southward at the end of Spring, with

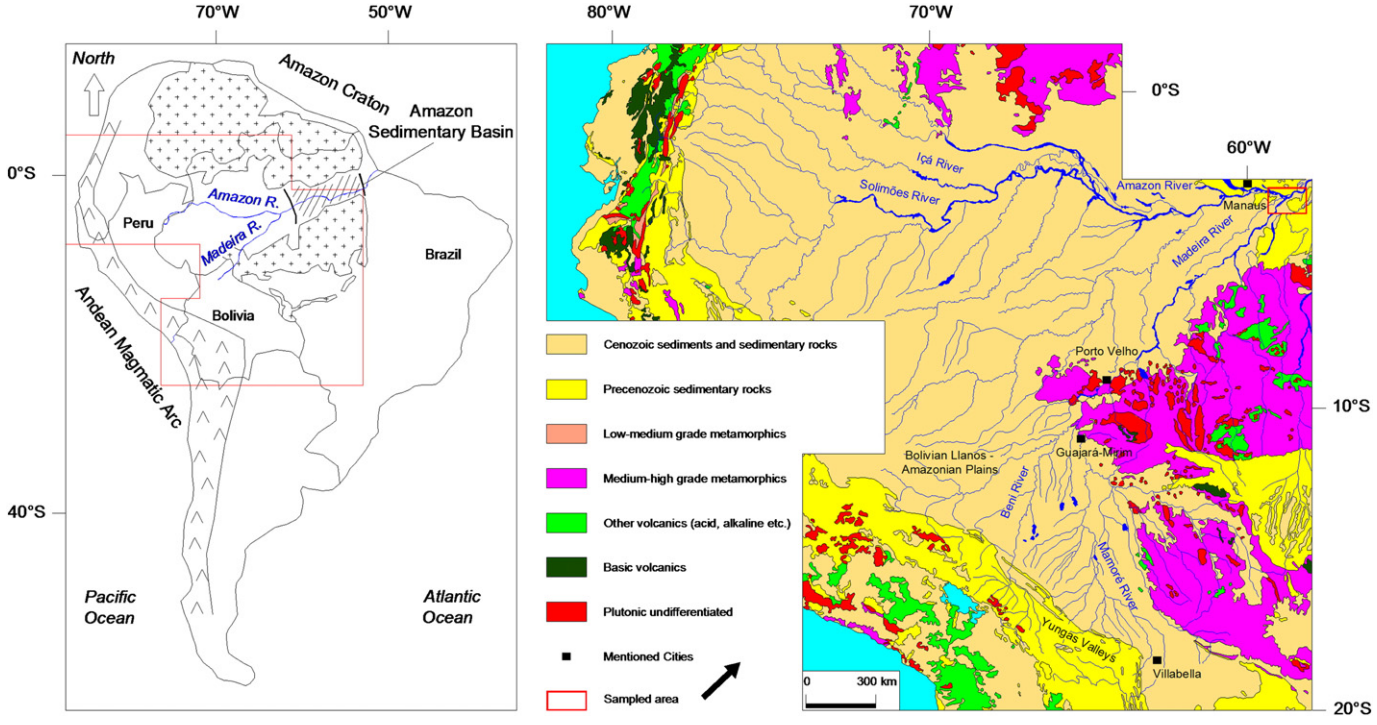

Fig. 1. Location and geology of the study region. Adapted from Schobbenhaus and Bellizia (2001).

the main period of rains in the Amazon river watershed concentrated between January and July. In the Madeira river watershed, the rainy season begins in October, with a precipitation peak in January and February, and a dry period from June to August (ANA, 2014).

From west to east, four main geological provinces are crossed by the Amazon river watershed (upstream of the Madeira river mouth): Andes Magmatic Arc (Cenozoic), Amazonian plains (Quaternary), Amazon Sedimentary Basin (Palaeozoic–Mesozoic) and Amazon Craton (Precambrian) (Schobbenhaus and Bellizia, 2001). About 90% of the drainage area runs over the Amazonian plains, whereas 5% encompasses the Andean Magmatic Arc and the remaining is divided into the other two terrains (Faria et al., 2004). The Madeira river watershed covers three of these provinces, with drainage areas of 25% in the Andes, 48% in the Amazon Craton (Llanos), and the remaining 27% in the Amazonian plains (Hayakawa et al., 2010).

In the highlands of the Andean range, the river morphology of the Amazon watershed alternates between sinuous and straight reaches, and also single- to multi-channel divisions (Latrubesse et al., 2005). The channel pattern of the majority of the Amazon watershed, composed by the Solimões–Amazon system, is nowadays branched-anastomosed, with evidence of ridge-and-swale features of meanders over the bars and ancient fluvial terraces (Soares et al., 2010). Large areas around the main drainages are seasonally inundated during the rising stage of the rivers, corresponding to flat forested realms of the overbanks (*igarapés*). In the same areas, minor tributaries can suffer blockages by the development and migration of longitudinal bars in the main drainages, thereby forming lakes (Latrubesse and Franzinelli, 2005). In the Madeira watershed, the rivers are straight until they reach the Bolivian valleys of Llanos, where the morphology varies from straight to sinuous in a single channel, with wide meanders locally, where an area of about 150,000 km^2 is annually flooded (Roche and Fernandez, 1988). The valley width is 10–20 km, but can reach as much as 35 km in the central portion (Hayakawa et al., 2010).

The annual discharge of the Amazon river watershed presents huge variation conforming to the location of its main tributaries. According to Mangiarotti et al. (2013), for the period between 1995–2008, the Amazon river upstream to the Madeira river mouth (Manacapuru station, Solimões river) presents a mean discharge of about 102,000 $m^3\ s^{-1}$, but turns to 172,000 $m^3\ s^{-1}$ downstream (Óbidos station). The mean suspended load also varies between the stations, from 209 g/cm^3 (Manacapuru) to 149 g/cm^3 (Óbidos); this mentioned reduction would be caused by a downstream increase of the sedimentary accumulation rate on the Amazon river (Mangiarotti et al., 2013). Despite up to 95% of the Amazon river watershed covering Cenozoic sediments and sedimentary rocks, the streams draining the high slope and high precipitation Andean areas dominate the Amazon river's suspended sediment supply (Meade et al., 1985; Guyot et al., 2007). In turn, the annual discharge of the Madeira river is around 18,000 $m^3\ s^{-1}$, with a minimum of 2000 $m^3\ s^{-1}$ and maximum of 52,000 $m^3\ s^{-1}$ during the flooding period (Bourges and Hoorelbecke, 1995). In Villabella, the total sedimentary load of the river is estimated at 230×10^6 m^3/year, with 72% of the sediment load provided by the Beni river, and the remaining 28% by the Mamoré river (Bourges and Hoorelbecke, 1995; Guyot et al., 1999). The grain size distribution of the bedload sediments in the Bolivian watershed of the Madeira river demonstrates rapid deposition of the coarse fraction (>10 mm) as the river flows out of the Andean range and enters the Amazonian plains (Llanos) (Guyot et al., 1999).

3. Rocks and sediments drained by the Amazon and Madeira rivers

About 70% of the Amazon catchment area (upstream to the Madeira river mouth) is located in Brazil and drains Cenozoic sediments and sedimentary rocks of the Amazonian plains since the "Precordillera" of Peru and Colombia, where the common lithologies are argillites, arenites, siltites and unconsolidated muds, sands and gravels (Reis et al., 2006), but with a primary origin from Andean rocks (Fig. 1). Despite the Negro river draining large areas of the Amazon Craton with exposed Precambrian rocks, most of its sediment supply is apparently trapped in fluvial–bar complexes from its middle and lower portions (Mariuá and Anavilhanas) since the prevalence of an Andean signature in the Amazon (formerly Solimões) river remains in the suspended sediments downstream of the Negro mouth (Guyot et al., 2007; Viers et al., 2008; Govin et al., 2014). Only a minor (900,000 km^2) portion of the present Amazon river catchment upstream of the Madeira mouth corresponds to tributaries of the Andean uplands in Peru (65%), Colombia (30%) and Ecuador (5%). In Peru, the drained rocks range from Cambrian to Palaeogene, being dominated by sedimentary (limestones, arenites, mudstones) and volcanosedimentary (tuffs and pyroclasts in general) units, followed by volcanics (andesites, dacites), and few plutonics (tonalites) and low-grade metamorphics (schists) (Instituto Geológico Minero and Metalurgico — INGEMMET, 1995). In Colombia, the rocks vary from Mesoproterozoic to Jurassic, and are composed mainly of high grade metamorphics (amphibolites, granulites), limestones and granites (Tapias et al., 2007). The catchments in Ecuador cover Cretaceous to Miocene sedimentary rocks (shales, marls, red beds, arenites, evaporites), with very few tuffs (Longo and Baldock, 1982). The rock assemblage from Peru, Colombia and Ecuador is expected to source sands rich in feldspar grains and unstable heavy minerals such as pyroxenes and amphiboles, whereas in the Amazonian plains (Brazil) the expected assemblage would be enriched in stable components (quartz-rich sediments).

The rocks that are potential primary sources of sediments for the Madeira river can be grouped into three units from upstream to downstream. In the Upper Madeira river, rocks of its catchments (Beni and Mamoré rivers) on the Andean Cordillera are mainly represented by sedimentary units ranging from Ordovician to Palaeogene, but clearly dominated by lithologies of the Ordovician and Devonian periods (Fig. 1). Arenites, carbonates and shales are dominant in the Ordovician area, and coarse sandstones (arkose and lithic), lutites (mudstones and shales) and fine sandstones are dominant in the Devonian region (Salinas et al., 1989; Pérez et al., 1996; Oca, 1997; Schobbenhaus and Bellizia, 2001). Minor lithologies of the all other periods include also conglomerates, diamictites, marls, mudstones, tuffs, and isolated igneous (volcanic and plutonic) of acid to basic composition, eventually alkaline. Locally, some low-grade metamorphism is evident in any of the mentioned sedimentary rocks (Oca, 1997). This rock assemblage is expected to source sands rich in lithic and feldspar grains as well as unstable minerals such as pyroxenes and amphiboles.

The middle portion of the Madeira river encompasses Quaternary alluvial deposits (Amazonian plains), starting downstream of the Bolivian "Precordillera" (Villabella) (Fig. 1). There, gravelly to muddy sands are present and partially correspond to ancient terraces and floodplains of the Beni and Mamoré rivers. This alluvial plain is build by trapping of sediments principally sourced by Andean tributaries. However, catchments on the east side are partially flowing over terrains of the cratonic Brazilian Shield (Amazon Craton), and then predominantly downstream Guajará-Mirim (Brazil). In this area, the Amazon Craton is composed mainly of medium-to-high grade metamorphic rocks (granitoid gneisses, amphibolites and schists), and by acid igneous rocks (granites) that are sometimes alkaline (Tassinari and Macambira, 2000). In minor amounts, other lithologies include quartzite, calcisilicates, diorites and few remains of sedimentary (sandstones, siltites, shales, conglomerates) and volcanic (basalt) rocks of the Parecis Basin are present in the southwestern Amazon Craton (Siqueira, 1989; Ferreira et al., 2006; Bahia et al., 2007). The lower sector of the Madeira river starts downstream Porto Velho (Brazil) in the Amazonian plains, running over its own ancient fluvial deposits and Cretaceous to Neogene rocks of the Amazon sedimentary basin (Eiras et al., 1994; Ferreira et al., 2006). These rocks are red sandstones, siltites, conglomerates, shales and argillites (Daemon, 1975; Monsch, 1998; Wesslingh et al., 2001; Rossetti and Neto, 2006). Also, rivers draining cratonic Precambrian rocks reach the Madeira river downstream of Porto Velho.

4. Methods

4.1. Sampling and measuring of channel bathymetry

The sampling area comprehends the downstream sector of the Madeira river channel and the Amazon main channel upstream and downstream of the Madeira river mouth (Fig. 1). Twenty-nine sediment samples were collected in the lower Madeira river and Amazon river around the Madeira river mouth, from exposed sand bars or in the mid portion of channels using a grab sampler. The Amazon river samples comprise 5 samples collected upstream and 13 samples collected downstream. The remaining 8 samples were collected in the Madeira river. The water depth in the sampling sites ranged from 2.5 to 34 m (mean of 14 m).

To the channel morphology at the sampling points, 6 bathymetric profiles were constructed using sonar with coupled GPS (Garmin sonar model GPSMAP 541). Data consisting of longitude/latitude/water depth were recorded during the 2011 dry season (November) along a transverse line roughly perpendicular to the main channel. To draw the profiles, a best-fit line was adjusted to each dataset and the points were projected perpendicularly to this line. Water depth profiles were used to constrain the morphology of main river channel, allowing the identification of secondary channels and underwater sediment bars (shoals).

4.2. Heavy mineral analysis

To perform the heavy mineral analysis, samples were wet sieved to acquire the 180–250 μm grain size. Heavy minerals were separated in lithium metatungstate solution (2.85 g/cm^3) using paper funnels to remove the light floating fraction. The non-magnetic fraction was mounted onto glass sides using Canada balsam as medium for study under a polarising microscope. Where possible, one hundred non-micaceous transparent grains plus opaque grains were identified and counted using the ribbon counting method (Galehouse, 1971). The content of each mineral type was calculated as percentage of grains within the assemblage.

4.3. Optically stimulated luminescence (OSL) sensitivity measurements

The OSL characteristics of quartz and feldspar have been studied intensely during the last years due to their role for dating of sediment deposition (Aitken, 1998; Rhodes, 2011). Feldspars usually have intense luminescence (blue and ultraviolet emissions) when stimulated by infrared light (Duller, 1991). The absence of infrared stimulated luminescence (IRSL) in quartz allows its discrimination from feldspars (Duller, 2003). Quartz from rocks and sediments commonly presents huge variations in OSL sensitivity, which is the light intensity emitted per unit of radiation dose (Sawakuchi et al., 2011). Laboratory experiments have shown that cycles of irradiation and bleaching enhance the OSL sensitivity of quartz (McKeever et al., 1996; Li, 2002; Moska and Murray, 2006; Koul and Chougaonkar, 2007). Pietsch et al. (2008) demonstrated that fluvial transport can increase the OSL sensitivity of quartz grains through natural cycles of transport (sunlight exposure = bleaching) and deposition (irradiation under burial and build-up of a luminescence signal). Despite high variation of the OSL sensitivity of quartz in source rocks, the increase in OSL sensitivity during sedimentary transport would surpasses the sensitivity inherited from source rocks (Sawakuchi et al., 2011). Thus, the OSL sensitivity would discriminate quartz grains with different erosion-deposition histories, allowing its use as a provenance proxy (Fitzsimmons, 2011; Sawakuchi et al., 2012; Lü et al., 2014).

In this study, we combined OSL measurements using blue and infrared stimulation to obtain proxies for sediment discrimination using sand grain size. OSL sensitivity measurements were performed to generate indices potentially capable of estimating the proportion of feldspar grains and the erosion–deposition history of quartz grains, as proposed by Pietsch et al. (2008) and Sawakuchi et al. (2011, 2012). For this, the light mineral fraction (180–250 μm, density < 2.85 g/cm^3) obtained during heavy mineral separation was used. The OSL measurements were carried out in a Risø TL/OSL DA-20 reader equipped with a built-in beta source (dose rate of 0.088 Gy/s), bialkali PM tube (Thorn EMI 9635QB) and Hoya U-340 filters (290–340 nm). For each sample, we measured 12 multigrain aliquots with the same volume, comprising around 150 to 200 sand grains per aliquot. The OSL measurements sequence was performed in six steps: 1. optical bleaching using blue LEDs (stimulation during 100 s at room temperature, 90% LED power); 2. a given beta dose of 10 Gy; 3. pre-heating at 190 °C for 10 s; 4. IR stimulation during 300 s at 60 °C; 5. a first blue LED stimulation during 100 s at 125 °C; and 6. a second blue LED stimulation during 100 s at 125 °C.

Step 1 aimed to eliminate any residual natural luminescence signal (by the background and/or cosmic radiation). Step 4 (infrared stimulation, IR) measured the feldspar signal and bleached feldspar grains prior to blue-light stimulation for OSL measurements of quartz grains (steps 5 and 6). Step 6 was used to determine the background for the OSL decay curve obtained during step 5. The luminescence sensitivity was represented by the integral of the initial 1 s of light emission (fast component-dominated signal) and total OSL decay curves. The integral of the first 1 s of light emission was used to represent the fast component-dominated signal (Choi et al., 2006) for IR and blue-light (BL) stimulated OSL decay curves. The sensitivity of the fast component was represented as percentage of the total OSL curve. The luminescence signals were used for calculation of three OSL indices, whose definition and significance are presented in Table 1.

5. Results

5.1. Bathymetric profiles

In the study area, the Amazon and Madeira rivers presented contrasting bathymetric profiles concerning depth, width, and bottom morphology (Fig. 2). Between profiles A1 and A2 (separated by 40 km), the Amazon river narrows its channel from 4700 m to 2500 m width, accompanied by increase of the mean depth from −18 to −33 m. In the A1 profile, there is a “central plateau” where the mean depth is −8 m, probably corresponding to an subaqueous extension of the upstream emerged mid-channel bar (Onças Island, Fig. 3). Underwater bars share the main channel in secondary channels.

Despite the same distance separating its first (M1) and last (M4) profile, more dramatic changes occur in the Madeira river. In the Madeira river, the channel initially widens from 1050 m to 2000 m with reduction of the mean depth from −14.6 m to −6.6 m (M1 to M2); then, the channel reduces its width to 800 m and increases the mean depth to −32 m (M2 to M4). The channel narrowing and deepening favour the development of a single chute confining the bedload transport. From upstream (M1) to downstream (M4), these profile changes include a general increase of the bottom asymmetry characterised by smoother margins in the southern sectors.

5.2. Heavy minerals

The collected samples for heavy mineral analysis are silty sands, being the sand fraction dominated by fine and very fine sand particles. The heavy mineral analysis involved the counting of almost 5000

Table 1
OSL indices used to measure the feldspar content and sensitivity of feldspar and quartz grains. IR and BL are infrared and blue stimulated luminescence respectively.

OSL index	Calculation	Significance
Fast IR-BL	First 1 s IR/First 1 s BL	Feldspar-to-quartz grains ratio
Fast IR	(First 1 s IR/300 s IR) × 100	Sensitivity of feldspar grains
Fast BL	(First 1 s BL/100 s BL) × 100	Sensitivity of quartz grains

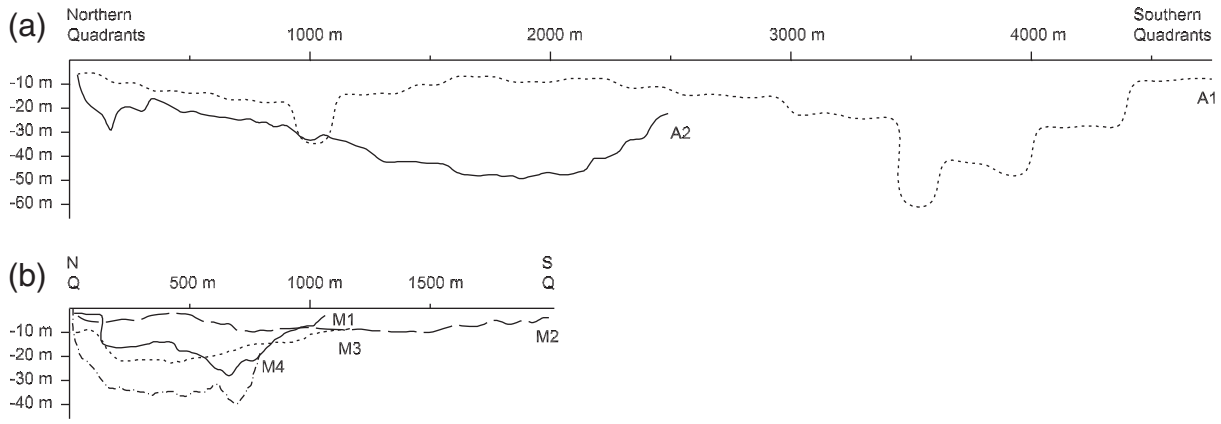

Fig. 2. Bathymetric profiles of the (a) Amazon and (b) Madeira rivers, with numbers in ascending order from upstream to downstream. The vertical exaggeration is 10×. See Fig. 3 for location.

transparent grains, of which about 30% on average were chemically-altered unidentified grains (here termed alterites, in the sense of van Andel, 1958). The identified assemblages in decreasing abundance (average of all samples) were: augite (19.9%), hypersthene (15.1%), andalusite (15.1%), green hornblende (14.7%), garnet (4.9%), diopside (4.4%), sillimanite (4.4%), brown hornblende (3.9%), staurolite (3.6%), kyanite (3.4%), zircon (2%), tourmaline (1.7%) and clinozoisite (1.5%). Other identified grains, with less than 1% on average (traces), were titanite, monazite, titanaugite, aegirine, epidote, rutile, cassiterite and brookite (Figs. 3, 4, Table 2).

Significant differences in the distribution of the four most abundant heavy minerals were found among the studied samples (Figs. 3, 5). Most of the samples from the Madeira river show a high content of andalusite (mean of 28.3%, median of 19.4%), while the Amazon river upstream of the Madeira mouth has a high content of hypersthene (mean of 27.6%, median of 17.9%) and augite (mean of 20.9%, median of 18%) (Fig. 3). Green hornblende is abundant in the sands from these two rivers, but with a slightly higher content in the Madeira river (mean of 20.6%, median of 8.8%). In the downstream portion of the Amazon river, the effect of mixing promoted by the sedimentary input of the Madeira river is clear, especially tracked by the presence of andalusite (mean of 7.1%, median of 2.1%), which occurs in low content upstream the Madeira river mouth. However, content of andalusite downstream Amazon also presents a large variation (0–42.3%) of mean percentage between samples, suggesting poor mixing between the Amazon and Madeira rivers sands in the studied sector (Fig. 6).

5.3. OSL sensitivity

The luminescence sensitivity measurements are represented by averages obtained for 12 aliquots of each sediment sample. The data are grouped into Upstream Amazon, Madeira and Downstream

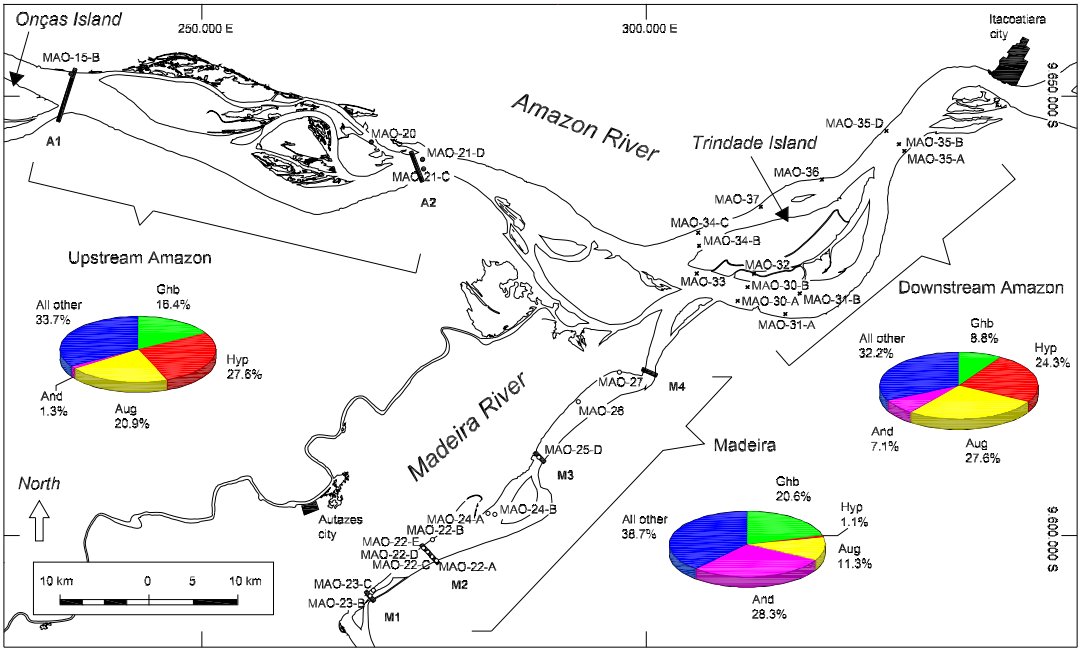

Fig. 3. Location of the sampled sites of the study. Full circles refer to upstream Amazon river samples (with reference to the Madeira river mouth), open circles refer to Madeira river samples, and X symbols refer to downstream Amazon river samples (with reference to the Madeira river mouth). The pie charts represent the average percent of the main heavy minerals of all samples from each of the three indicated fluvial stretches. Symbols of the graphics: Ghb = green hornblende; Hyp = hypersthene; Aug = augite; And = andalusite. The black stripes identified by the letters in bold font A (Amazon) and M (Madeira) indicate bathymetric profiles. See text for explanation.

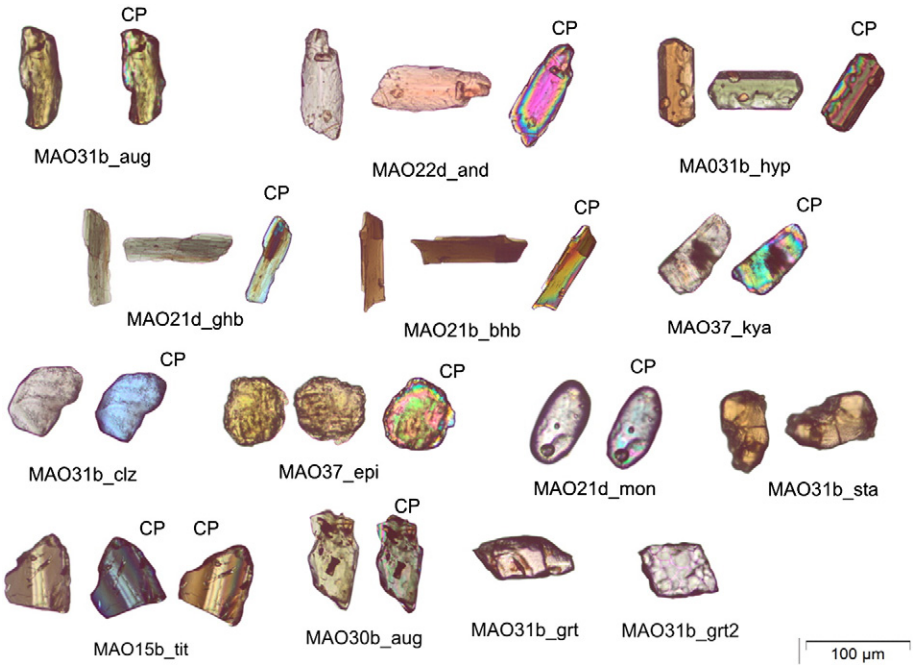

Fig. 4. Selected examples of heavy minerals from the sands of Madeira and Amazon rivers. The three last letters in the code below represent a mineral (see Table 2). Images in crossed polarisers are indicated by CP above.

Amazon. Luminescence data show a tendency of decreasing IRSL signal with increasing quartz OSL sensitivity (Fig. 7a). When compared to the Amazon river sands, the sands of the Madeira river show relatively lower feldspar content (low IRSL signal) and quartz with higher OSL sensitivity. The Amazon river sands have almost similar feldspar and quartz signatures upstream and downstream. It is interesting to note that some samples of the Madeira river have luminescence characteristics very close to those of the Amazon sands. Because of this, a better

Table 2
Percentage of heavy minerals identified in the samples. Symbols: Ghb = green hornblende; Bhb = brown hornblende; Hyp = hypersthene; Aug = augite; Dio = diopside; Grt = garnet; And = andalusite; Kya = kyanite; Sil = sillimanite; Sta = staurolite; Clz = clinozoisite; Tou = tourmaline; Zir = zircon; Traces = titanite, monazite, titanaugite, aegirine, epidote, rutile, cassiterite, and brookite. Alterites refer to chemically-altered unidentified grains (van Andel, 1958); n = total number of grains in each sample.

		Unstables[a]						Metastables					Ultrastables			
Sample	n	Ghb	Bhb	Hyp	Aug	Dio	And	Grt	Kya	Sil	Sta	Clz	Tou	Zir	Traces	Alterites
MAO-15-B	161	21.4	5.3	20.6	8.4	4.6	1.5	3.1	0.0	0.0	4.6	0.0	1.5	0.0	1.5	26.0
MAO-20	129	4.3	3.3	15.2	1.1	12.0	1.1	2.2	1.1	2.2	3.3	0.0	1.1	0.0	1.1	51.1
MAO-21-C	149	10.5	1.9	34.3	27.6	0.0	0.0	7.6	0.0	1.9	0.0	0.0	0.0	1.0	1.0	14.3
MAO-21-D	166	13.2	5.0	9.9	32.2	6.6	0.8	3.3	0.8	2.5	2.5	0.8	0.8	0.0	5.8	14.9
MAO-22-A	222	35.9	3.9	0.0	1.6	1.6	8.6	1.6	0.8	0.8	1.6	2.3	2.3	0.0	4.7	32.0
MAO-22-B	159	11.0	1.4	1.4	0.0	0.0	26.0	0.0	2.7	2.7	1.4	1.4	0.0	1.4	0.0	50.7
MAO-22-C	272	4.1	0.0	0.0	4.1	1.4	20.3	1.4	7.4	4.7	0.7	0.7	0.7	0.7	3.4	50.0
MAO-22-D	166	13.1	3.3	0.0	3.3	0.0	4.9	8.2	1.6	3.3	0.0	1.6	4.9	4.9	3.3	42.6
MAO-22-E	435	28.7	5.7	0.5	4.3	1.0	8.1	0.5	1.4	3.3	1.9	0.5	1.9	0.0	0.0	40.2
MAO-23-B	186	6.1	2.0	2.0	4.0	0.0	23.2	0.0	11.1	4.0	0.0	5.1	2.0	0.0	2.0	36.4
MAO-23-C	92	21.7	4.3	0.0	0.0	4.3	4.3	8.7	0.0	0.0	0.0	0.0	0.0	21.7	0.0	34.8
MAO-24-A	193	0.0	0.0	0.0	16.7	0.0	0.0	0.0	0.0	0.0	0.0	0.0	0.0	0.0	0.0	83.3
MAO-24-B	175	4.3	1.1	1.1	0.0	0.0	34.4	4.3	1.1	8.6	3.2	2.2	1.1	3.2	2.2	32.3
MAO-25-D	117	6.1	3.0	1.5	0.0	3.0	21.2	0.0	3.0	1.5	1.5	1.5	1.5	0.0	1.5	53.0
MAO-26	187	9.3	2.1	1.0	2.1	0.0	18.6	3.1	4.1	5.2	1.0	2.1	2.1	0.0	5.2	41.2
MAO-27	163	8.3	1.2	0.0	1.2	0.0	22.6	2.4	2.4	8.3	2.4	0.0	2.4	0.0	1.2	45.2
MAO-30-A	182	3.0	3.0	0.0	0.0	0.0	22.2	0.0	5.1	10.1	4.0	0.0	1.0	1.0	2.0	47.5
MAO-30-B	154	7.5	0.8	19.2	34.2	0.0	3.3	4.2	0.8	0.0	1.7	0.0	0.8	0.0	5.8	20.8
MAO-31-A	226	12.2	3.3	5.7	13.8	2.4	17.1	3.3	3.3	4.1	0.8	3.3	0.0	2.4	1.6	26.8
MAO-31-B	221	6.5	1.4	31.9	25.4	0.7	0.0	7.2	0.0	0.0	2.9	0.0	0.0	0.0	3.6	20.3
MAO-32	131	6.9	2.9	11.8	8.8	21.6	0.0	2.9	0.0	0.0	11.8	1.0	1.0	0.0	0.0	30.4
MAO-33	72	5.3	1.8	15.8	8.8	5.3	1.8	0.0	1.8	1.8	1.8	0.0	1.8	0.0	3.5	49.1
MAO-34-B	158	7.0	0.9	20.2	24.6	0.0	0.9	3.5	0.9	1.8	1.8	0.0	0.9	0.0	3.5	33.3
MAO-34-C	142	2.2	1.1	35.5	38.7	0.0	3.2	3.2	0.0	2.2	1.1	2.2	0.0	1.1	1.1	8.6
MAO-35-A	170	0.8	4.1	17.4	33.9	0.8	1.7	1.7	0.8	1.7	3.3	0.8	0.0	0.0	4.1	28.9
MAO-35-B	90	3.4	1.7	16.9	30.5	1.7	5.1	6.8	1.7	3.4	1.7	0.0	0.0	0.0	3.4	23.7
MAO-35-D	236	8.0	1.1	16.0	2.1	11.2	2.1	5.3	2.7	2.7	9.0	1.1	1.1	0.0	4.8	31.9
MAO-36	129	11.3	4.7	16.0	23.6	1.9	0.0	5.7	0.9	0.0	1.9	0.9	0.9	0.0	0.9	30.2
MAO-37	151	7.3	3.7	30.5	28.0	0.0	2.4	11.0	2.4	0.0	2.4	0.0	0.0	0.0	3.7	8.5

[a] Heavy mineral stability simplified from Pettijohn et al. (1972).

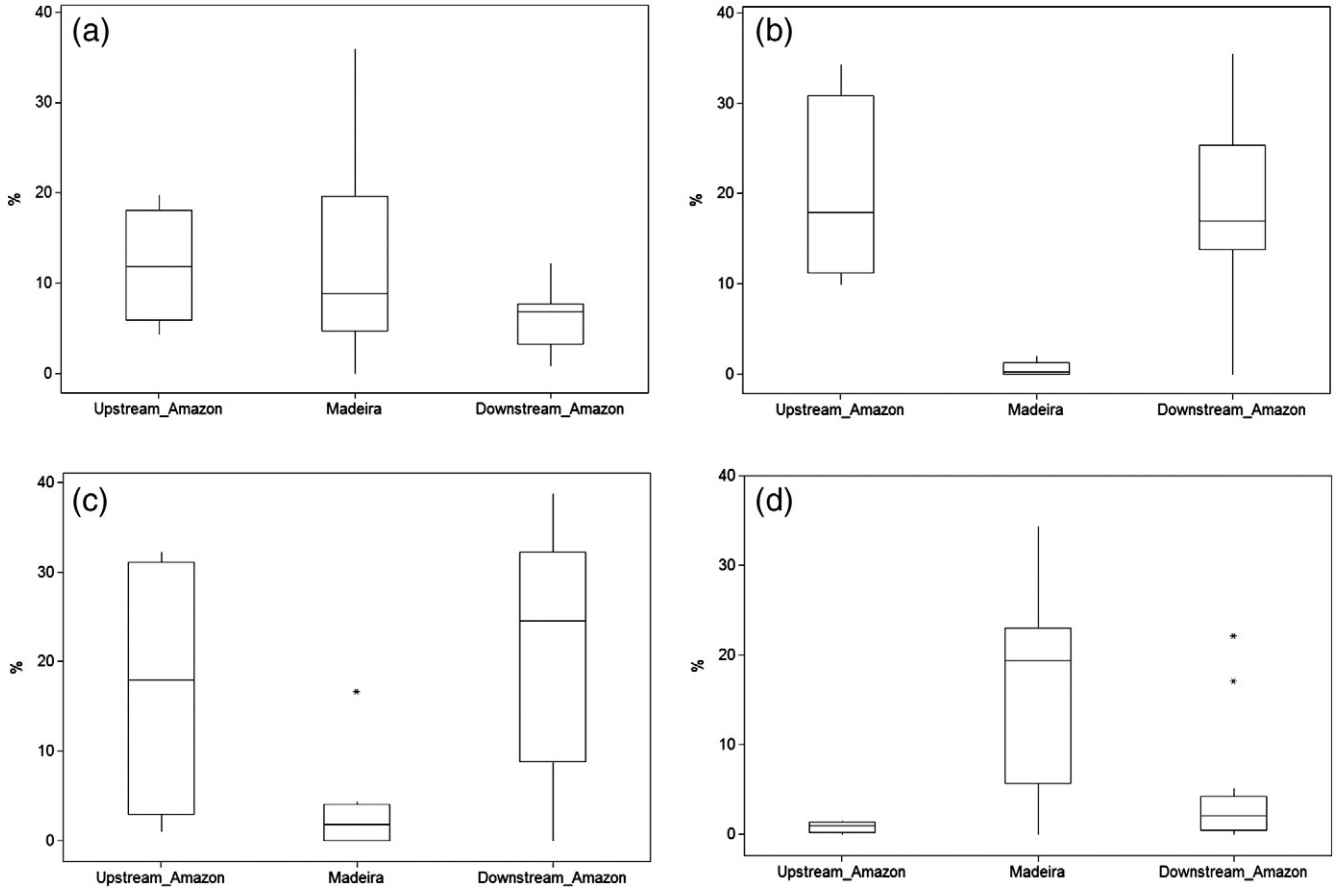

Fig. 5. Boxplot for the average percentage of the four most abundant heavy minerals identified in three sectors of the Lower Madeira River region: green hornblende (a), hypersthene (b), augite (c) and andalusite (d). The asterisks represent outlier values.

discrimination between Madeira and Amazon river sands, for provenance purposes, is acquired by plotting andalusite content versus IRSL signal (feldspar content) (Fig. 7b). End-member Amazon sands show higher feldspar and lower andalusite contents compared to Madeira end-member sands (Fig. 4). This comparison also suggests that mixed sands occur in the Amazon river downstream the Madeira as well as in the lower reach of the Madeira river.

6. Discussion

6.1. Sand source rocks

The sands from the Amazon river upstream of the Madeira river mouth stand out due to their high content of augite (24.1%) associated with hypersthene (27.6%) and brown (hastingsitic?) hornblende. This

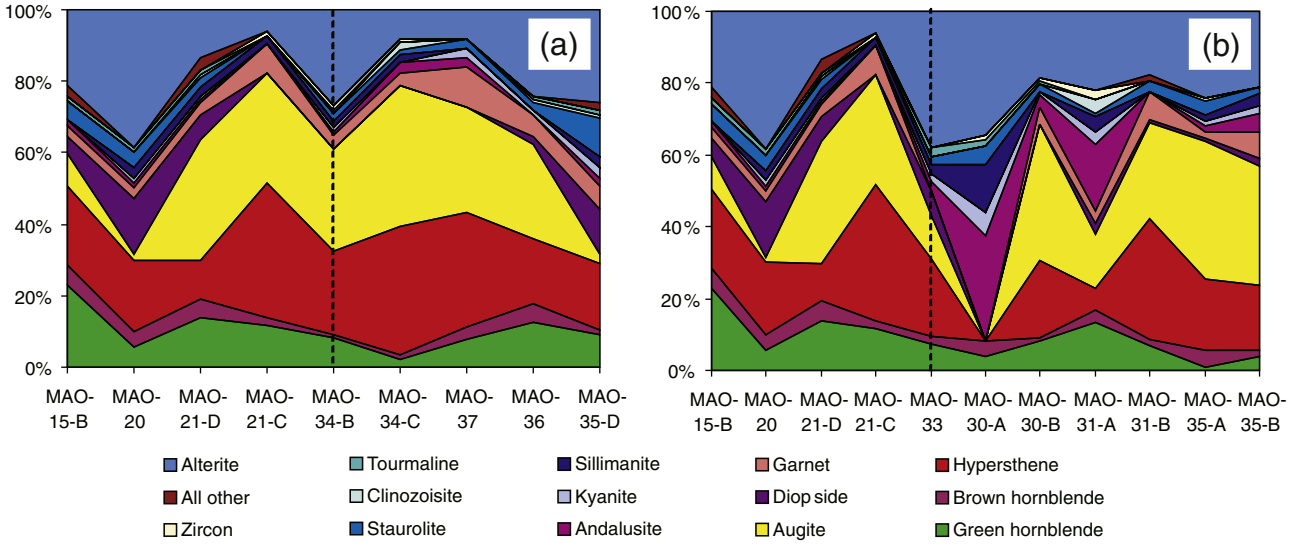

Fig. 6. West to east (left-right) distribution of heavy minerals of the sands of Amazon river in the Lower Madeira river region, at north (a) and south (b) from the Trindade Island. The dashed lines indicate the point of entrance of Madeira river sands on the Amazon river.

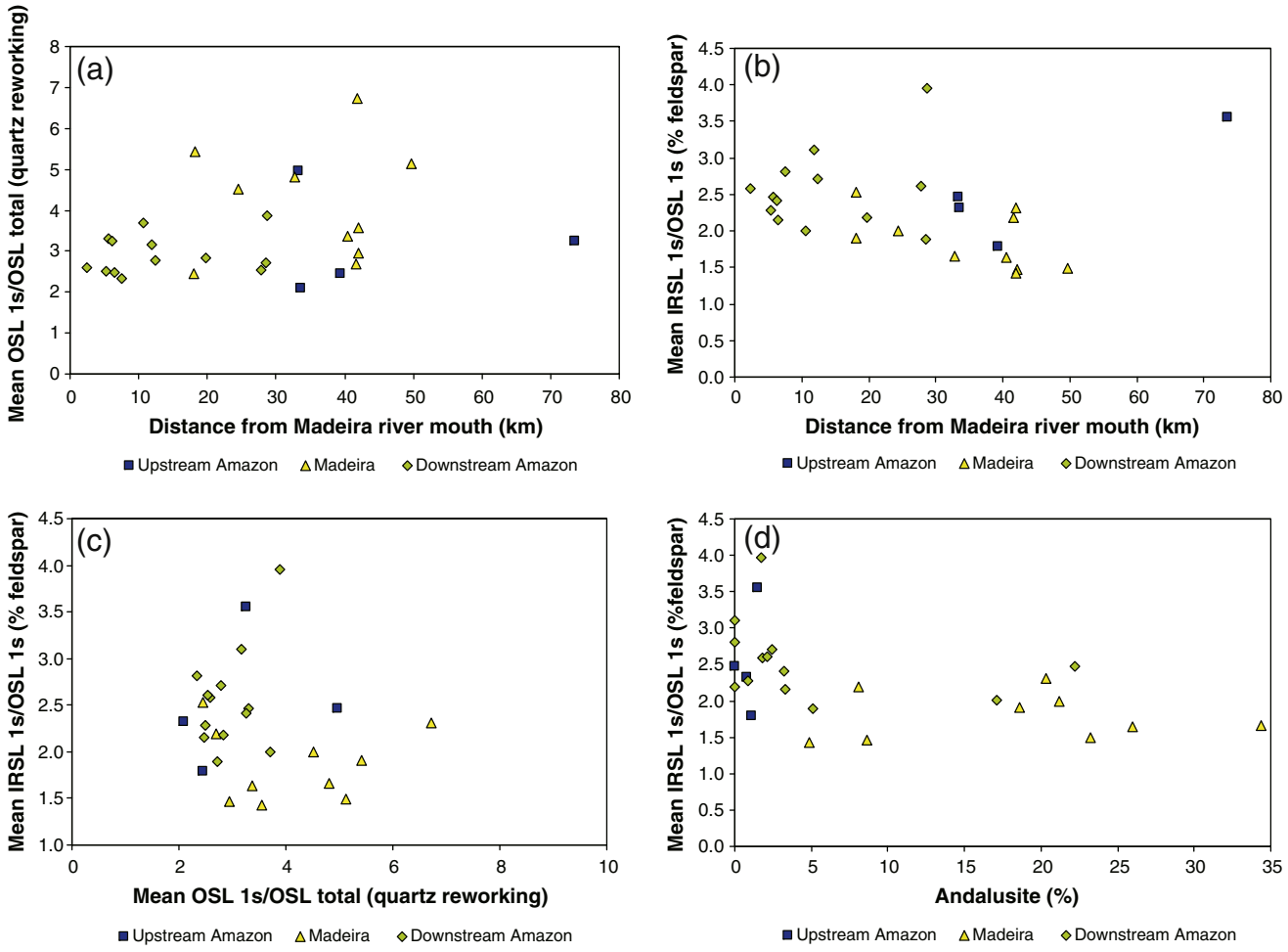

Fig. 7. OSL indices for sensitivity and feldspar content. (a) Variation of the quartz reworking along the three sectors (with reference to the Madeira river mouth). (b) Percentage of feldspar along the three sectors (with reference to the Madeira river mouth). (c) Scatterplot for quartz reworking versus percentage of feldspar. (d) Scatterplot for the percentage of andalusite versus the percentage of feldspar.

heavy mineral assemblage suggests a high proportion of basic igneous rocks in the sediment source area. Despite the presence of augite and (less) hypersthene, the Madeira river also has a high content of andalusite (26.1%) and associated metamorphic minerals, such as sillimanite, staurolite and kyanite, suggesting a significant contribution of medium-to-high grade para-derived metamorphic rocks. Green hornblende also has a high content in Madeira river sands suggesting metamorphic source rocks instead of volcanic. The medium-to-high grade metamorphic minerals (andalusite–sillimanite–kyanite–staurolite) occurring in high content in the Madeira river sands would be derived from a cratonic rock assemblage (Amazon Craton).

Viers et al. (2008) show that the suspended sediments of the Solimões river (Amazon upstream to the Negro river) have a provenance much more dominated by volcanic Andean rocks than in the suspended load of the Madeira river. Thus, Andean sediments would be indirectly sourced by areas in the foreland zone, considering that the restricted highland Andean areas are drained by the present fluvial system. Based on this, we interpret that the Andes Range (primary rocks and foreland sediments) and the Amazon Craton comprise the two end-member source rocks assemblages for the sands reaching the downstream portion of the Madeira river. High content of medium-to-high grade metamorphic heavy minerals points out that cratonic rocks are more important than Andean rocks as sources of sands for the lower Madeira river. Thus, the dominance of cratonic source rocks would differentiate the Madeira river sands from the Amazon river sands, which in turn would be dominated by the Solimões river sands, having a higher allochtonous contribution derived from Andean igneous rocks as suggested by elevated contents of augite, hypersthene and hornblende. This interpretation is also supported by the luminescence characteristics of the sands. The sands from the Madeira river have a lower feldspar content and quartz with higher OSL sensitivity compared to the sands from the upstream Amazon river (Fig. 7). Therefore, the relatively higher maturity of the Madeira river sands, as indicated by the lower feldspar content and quartz with longer erosion–deposition history, points out to a greater input of sediments derived from cratonic source rocks, despite heavy minerals indicating some contribution from Andean rocks.

6.2. Sand and mud decoupling and implications for provenance analysis

Heavy minerals and luminescence of feldspar and quartz indicate cratonic areas as the major source for sand of the lower Madeira river. However, suspended sediments are composed mainly of the combined clay minerals smectite–illite–chlorite, indicating that Andean rocks and their derived reworked sediments dominate the supply of fine grained sediments (Guyot et al., 2007). Thus, there would be a decoupling between the supply of sand and mud (silt and clay) of the Madeira river. The prevalence of cratonic sources of sand can be related to trapping of Andean sands at the foreland zones in Beni and Mamoré rivers catchments. Smectite–illite–chlorite are also the main minerals in the fine-grained suspended sediments of the Amazon river upstream of the Madeira river (Guyot et al., 2007). Thus, the sand and mud supplies here have similar sources, pointing to a coupled sand and mud supply system and absence of zones for selective trapping of coarser size

fractions. The trapping of coarser Andean sediments in the upper sectors of the catchment differentiates the Madeira river from the Solimões river.

The sands supplied by the Madeira river to the Amazon river can be tracked by their elevated content of andalusite (mean of 7.1%), and lower content of feldspar and quartz with higher OSL sensitivity when compared to the upstream Amazon river sands (mean of 1.1% of andalusite). Sands with these characteristics predominate south of Trindade Island in the Amazon river channel, where a plume of sediments from the Madeira river can be seen in aerial and satellite images, especially during the flooding period between December and March (Fig. 8). Sands rich in augite, hypersthene, feldspar and low OSL sensitivity quartz, characterising a more typical Andean signature, occur in the channel north of Trindade Island. Despite that sands from the Madeira river can be tracked into the Amazon river (Fig. 6), stabilised bars and banks within the Amazon river channel hamper the mixing of sands from both rivers. Water depth profiles across the Amazon river show secondary channels separated by longitudinal sediment bars (Fig. 2). This morphology could promote a confined transport of sand in secondary channels within the main river channel, inhibiting the mixing between Amazon upstream sands and sands supplied by the Madeira river. This can explain the significant variation in composition observed among sediment samples collected across the Amazon river channel (samples 35A, B, D), which has multiple channels separated by wide sediment bars.

In provenance studies, both initial mixture of sediment grains from different source rocks and posterior modifications of the original mineral assemblage by abrasion and sorting during transport, as well as by weathering or diagenetic solution after deposition, make it difficult to determinate primary source rocks of sediments (Pettijohn et al., 1972; Pettijohn, 1975; Morton and Hallsworth, 1994, 1999). Heavy mineral analysis is an important instrument in sand provenance studies, because most heavy minerals are restricted to specific source rocks capable to provide distinguishable differences among sediment source areas (Sevastjanova et al., 2012). Several works have suggested potential source rocks for the most common heavy minerals (Pettijohn et al., 1972; Pettijohn, 1975; Mange and Maurer, 1991). Heavy minerals indices based on pairs of minerals with similar hydrodynamic and stability properties (physical and chemical) have been created to outline modifications imposed in the assemblage during the sedimentary cycle, i.e., due to factors as transport, weathering and diagenesis (Hubert, 1962; Morton and Hallsworth, 1994, 1999; Guedes et al., 2011) and be a provenance proxy. In this respect, zircon and rutile, which are almost absent in many of the studied samples here, are two of the most used minerals (Belousova et al., 2002; Dickinson and Gehrels, 2003; Zack et al., 2004; Griffin et al., 2006; Triebold et al., 2007; Howard et al., 2009; Tanaka et al., 2009; Bahlburg et al., 2010; Meinhold, 2010; Clements and Hall, 2011; Guedes et al., 2011), but several others like tourmaline, amphiboles and even Fe–Ti oxide opaques are also used (i.e., Mange-Rajetzky, 1981; Cawood, 1990, 1991; Basu and Molinaroli, 1991; Morton et al., 1994; Mange and Morton, 2007; Nascimento et al., 2007). Even though heavy mineral indices can overcome the difficulties caused by factors of the sedimentary cycle (Morton and Hallsworth, 1994, 1999), they can introduce a positive or negative bias for specific source rocks. For example, soft rocks like sedimentary and schists could be more suitable to release higher amounts of specific minerals during the physical weathering in the source. Furthermore, although heavy mineral analysis is a powerful tool in tracking "primary" provenance (source rocks), the "secondary" provenance (i.e., the provenance of sediments from two rivers that are both distant from it sources) could be complicated based on estimation of the relative contribution from each feeder system, or when the final heavy minerals assemblage is very similar. As a result of these difficulties, better results could be obtained by OSL sensitivity analysis because it involves broader spectra of the grains, as long as there are significant differences between cycles of burial/solar exposure of the sands from each feeder system.

Significant changes in sediment composition and texture are expected during transport along large tropical fluvial systems such as the Amazon river and its tributaries, which drain areas under strong tropical weathering. On the other hand, sediment recycling that occurs when sediments are eroded from temporary storage, reveals important aspects of their dynamics. So far, changes in sand-forming minerals (quartz and feldspar) occurred during transport through continental scale tropical river systems such as the Amazon are poorly studied. Despite transport for more than 1500 km from their primary source rocks, the studied sands of the Amazon river are very rich in unstable grains such as feldspars, pyroxenes and amphiboles. This agrees with the significant quantity of unstable heavy minerals observed in sands of the lower Amazon river (Vital et al., 1999) and suggests that weathering

Fig. 8. Satellite image depicting the sedimentary plume of the Madeira river delivered to the Amazon river and persisting for more than 40 km downstream. Landsat 5 image, path/row 230/62, acquired in 14/07/2008. Colour composite RGB = TM3/TM2/TM1.

within the river system can have a minor role in sand composition. A similar result was found by Sevastjanova et al. (2012) in the tropical areas of the Malay Peninsula and Sumatra (SE Asia). In the Amazon river, the preservation of the primary source rocks' mineralogy indicates a fast transfer of sands from weathered rocks in uplands to the Amazon river plain. The Amazon sands are rich in some unstable minerals with relatively low hydraulic equivalence as andalusite, augite and hornblende, and the relative proportion of these minerals vary regionally according to discharge and sediment yield from the different tributaries. This characteristic indicates the major role of Amazon tributaries in determining sand composition, and evidences the scarce effect of weathering and hydraulic sorting over river sand mineralogy.

The weathering of sand within the river system would be limited due to the short storage time in floodplains or stabilised bars. This is supported by the low OSL sensitivity of quartz grains from the Amazon river, indicating that sand transport does not increase quartz luminescence sensitivity due to cycles of erosion and deposition, as shown in other studies (Pietsch et al., 2008; Sawakuchi et al., 2011). In the Lower Madeira and Amazon rivers, the seasonal dynamics between flood and dry periods reworks the sands previously deposited on floodplain terraces and bars and banks in the interior of the channel. When comparing the sensitivity indices between the three sectors of the rivers (Upstream Amazon, Madeira, Downstream Amazon), it is notable that samples are very similar, regardless of fluvial stretch of origin, distance from the Madeira river mouth or even location in the channel (Figs. 7, 9). Because of this, the performed OSL sensitivity analyses on sands with limited range of grain size imply that Amazon and Madeira rivers, in the Lower Madeira river region, would have a very close sedimentary behaviour with respect it dynamic of transport and storage of sands (i.e., number of cycles and/or residence time of the grains in the bars). Likewise, some studies have demonstrated that Amazon and Madeira rivers have similar turbidity (>100 NTU; Silva et al., 2010; Bernin et al., 2013), which can be critical in the penetration of sunlight and therefore the optical bleaching of sands (i.e., Sawakuchi et al., 2011).

Similar to the sensitivity indices, both rivers present unstable heavy mineral assemblages. This also presupposes that both mechanical abrasion along transport and chemical weathering during storage have been unable to modify significantly the initial mineralogy of sands from the rivers. Therefore, the found differences in the unstable heavy minerals' composition between the rivers would be related to differences on it sources. By extension, we interpret that the relatively high sensitivity of the Madeira river sands must be caused rather by differences on the source from its quartz. Hence, the time of storage would not be long enough for development of a significant luminescence signal, and/or abrupt erosion combined with deep turbid water channel would not promote efficient solar exposure and bleaching of quartz grains. Thus, sands are transported long distances without increasing in quartz OSL sensitivity (Fig. 7a,b). In this case, the higher sensitivity of quartz from the Madeira river would be related to cycles of erosion and deposition inherited from ancient sedimentary rocks in the source areas. Therefore, OSL sensitivity of quartz in sands from the Madeira and Amazon rivers is a more a proxy for source areas than for sediment reworking within the fluvial system.

7. Conclusions

The heavy mineral analysis revealed an unexpected assemblage in the recent sands of the Amazon and Madeira rivers, enriched in unstable minerals like augite, hypersthene, hornblende and andalusite. This is in agreement with the relatively high content of feldspar grains in sands from both rivers. Considering that these two rivers drain tropical climate regions, supposedly unsuitable for the preservation of unstable minerals, our results indicate that the Amazon fluvial system is very competent in transporting sands from uplands with primary source rocks to lowlands in the Amazonian fluvial plain. The river sands upstream of the Madeira mouth are supplied mainly by the Solimões river, having a heavy minerals signature characterised by hypersthene and augite. These minerals point to a provenance from basic igneous rocks of the Andean Range. Despite an Andean provenance also being recorded in the Madeira river, high contents of andalusite, quartz with higher OSL sensitivity and lower content of feldspar highlight source areas of medium-to-high grade metamorphic rocks and/or sedimentary rocks from the Amazon Craton. Most of the Andean sand supply would be trapped in upstream tributaries of the Madeira river in foreland areas, increasing the relative contribution of sands from downstream source areas in the Amazon craton. Thus, a decoupling between the sand (cratonic > Andean) and mud (Andean >> cratonic) supply is proposed for the Madeira river.

In the Amazon river, zones clearly influenced by the Madeira river water discharge are enriched in sands with a provenance signature from the Madeira river (rich in andalusite, lower feldspar–quartz ratio and quartz with higher OSL sensitivity), whereas sands with a signature from upstream Amazon river (enriched in augite and hypersthene, higher feldspar–quartz ratio and quartz with lower OSL sensitivity) prevails in other parts of the Amazon channel. This pattern indicates poor mixing of sands in the confluence of the Amazon and Madeira rivers.

Acknowledgements

The authors would like to thank Johanna Méndez Duque, Luciana Nogueira and Thays Desirée Mineli by the careful preparation and measurement of the samples. We also like to thank Dr. Piotr Weckwerth and

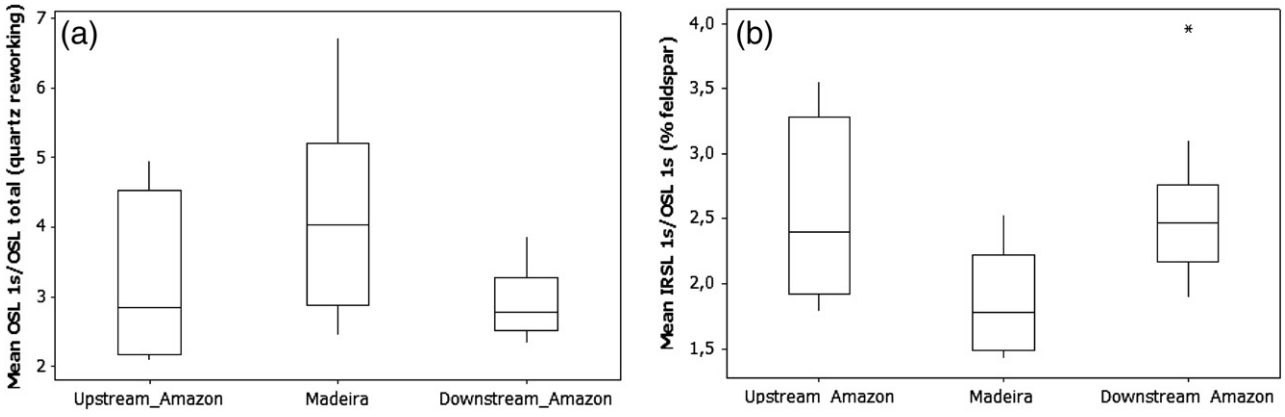

Fig. 9. Boxplots for the sensitivity indices of the three main Amazonian river sectors. (a) Index for quartz reworking. (b) Index for percentage of feldspar. See text for discussion. The asterisks represent outlier values.

an anonymous reviewer by the useful comments on the first version of the manuscript, and we are grateful to Dr. Jasper Knight (Editor) by the detailed corrections in the text. D.R.N.Jr. thanks *Conselho Nacional de Pesquisa Científica e Tecnológica* (CNPq) for a postdoctoral fellowship (Grant 159823/2011-0). This research was supported by *Fundação de Amparo à Pesquisa do Estado de São Paulo* (FAPESP, Grant 2011/06601-1). C.H.G. is a Research Fellow of CNPq (Grant 306294/2012-5).

References

Agência Nacional de Águas (Brazilian National Water Agency)., 2014. http://hidroweb.ana.gov.br/. Web site, (last accessed on 05/09/2014).
Aitken, M.J., 1998. An Introduction to Optical Dating. Oxford University Press, Oxford.
Allen, P.A., 2008. From landscapes into geological history. Nature 451, 274–276.
Allen, P.A., Allen, J.R., 2005. Basin Analysis — Principles and Applications. Blackwell Publishing, Oxford.
Bahia, R.B.C., Martins-Neto, M.A., Barbosa, M.S.C., Pedreira, A.J., 2007. Análise da evolução tectonossedimentar da Bacia dos Parecis através de métodos potenciais. Revista Brasileira de Geociencias 37, 639–649.
Bahlburg, H., Vervoort, J.D., DuFrane, A., 2010. Plate tectonic significance of Middle Cambrian and Ordovician siliciclastic rocks of the Bavarian Facies, Armorican Terrane Assemblage, Germany — U–Pb and Hf isotope evidence from detrital zircons. Gondwana Research 17, 223–235.
Basu, A., Molinaroli, E., 1991. Reliability and application of detrital opaque Fe–Ti oxide minerals in provenance determination. In: Morton, A.C., Todd, S.P., Haughton, P.D.W. (Eds.), Developments in Sedimentary Provenance Studies. Geological Society of London, pp. 55–65 (Special Publication 57).
Belousova, E., Griffin, W.L., O'Reilly, S.Y., Fisher, N.I., 2002. Igneous zircon: trace element composition as indicator of source rock type. Contributions to Mineralogy and Petrology 143, 602–622.
Bernin, H., Corrêa, A.C.S.S., Jordão, A.A., Checchia, T.E., Barbosa, I.S., Nascimento, C.R.V., 2013. Efeitos da barragem de Santo Antônio sobre a turbidez do rio Madeira: um estudo durante o período de enchimento do reservatório. 4th Scientific Meeting ORE-HYBAM, La Paz (Bolivia) ((www.ore-hybam.org) (last accessed on 03/11/2014)).
Blatt, H., 1967. Provenance determinations and recycling of sediments. Journal of Sedimentary Petrology 37, 1031–1044.
Bouchez, J., Gaillardet, J., France-Lanord, C., Maurice, L., Dutra-Maia, P., 2011. Grain size control of river suspended sediment geochemistry: clues from Amazon River depth profiles. Geochemistry, Geophysics, Geosystems 12, 1–24. http://dx.doi.org/10.1029/2010GC003380.
Bourges, J., Hoorelbecke, R., 1995. Variation du regime des aoulements dans le systéme ando-amazonien de Bolivie. In: Servat, E., LeBarbe, L. (Eds.), Régionalisation en hydrologie. ORSTOM, Paris, pp. 471–487.
Campbell Jr., K.E., Frailey, C.D., Romero-Pittman, L., 2006. The Pan-Amazonian Ucayali Peneplain, late Neogene sedimentation in Amazonia, and the birth of the modern Amazon River system. Palaeogeography, Palaeoclimatology, Palaeoecology 239, 166–219.
Carter, L., Orpin, A.R., Kuehl, S.A., 2010. From mountain source to ocean sink — the passage of sediment across an active margin, Waipaoa Sedimentary System, New Zealand. Marine Geology 270, 1–10.
Cawood, P.A., 1990. Provenance mixing in an intraoceanic subduction zone: Tonga Trench–Louisville Ridge collision zone, southwest Pacific. Sedimentary Geology 67, 35–53.
Cawood, P.A., 1991. Nature and record of igneous activity in the Tonga arc, SW Pacific, deduced from the phase chemistry of detrital grains. In: Morton, A.C., Todd, S.P., Haughton, P.D.W. (Eds.), Developments in Sedimentary Provenance Studies. Geological Society of London, pp. 305–321 (Special Publication 57).
Choi, J.H., Duller, G.A.T., Wintle, A.G., Cheong, C.-S., 2006. Luminescence characteristics of quartz from the Southern Kenyan Rift Valley: dose estimation using LM-OSL SAR. Radiation Measurements 41, 847–854.
Clements, B., Hall, R., 2011. A record of continental collision and regional sediment flux for the Cretaceous and Palaeogene core of SE Asia: implications for early Cenozoic palaeogeography. Journal of the Geological Society, London 168, 1187–1200.
Daemon, R.F., 1975. Contribuição para a datação da Formação Alter do Chão, Bacia do Amazonas. Revista Brasileira de Geociencias 5, 78–84.
Dickinson, W.R., Gehrels, G.E., 2003. U–Pb ages of detrital zircons from Permian and Jurassic eolian sandstones of the Colorado Plateau, USA: paleogeographic implications. Sedimentary Geology 163, 29–66.
Duller, G.A.T., 1991. Equivalent dose determination using single aliquots. Nuclear Tracks and Radiation Measurements 18, 371–378.
Duller, G.A., 2003. Distinguishing quartz and feldspar in single grain luminescence measurements. Radiation Measurements 37, 161–165.
Eiras, J.F., Becker, C.R., Souza, E.M., Gonzaga, F.G., Silva, J.G.F., Daniel, L.M.F., Matsuda, N.S., Feijó, F.J., 1994. Bacia do Solimões. Boletim de Geociências da Petrobrás 8, 17–45.
Everett, C.E., Rye, D.M., 2003. Source or sink? An assessment of the role of the old red sandstone in the genesis of the Irish Zn–Pb deposits. Economic Geology 98, 31–50.
Faria, M.S.G., Bahia, R., Almeida, M.E., Oliveira, M.A., 2004. Folha SA-20-Manaus e Folha SA-21-Santarém. In: Schobbenhaus, C., Gonçalves, J.H., Santos, J.O.S., Abram, M.B., Leão Neto, R., Matos, G.M.M., Vidotti, R.M., Ramos, M.A.B., Jesus, J.D.A. (Eds.), Carta Geológica do Brasil ao Milionésimo. Sistema de Informações Geográficas. Programa Geologia do Brasil. CPRM, Brasília (CD-ROM).
Ferreira, A.L., Almeida, M.E., Reis, N.J., Riker, S.L.R., Rizzotto, G.J., Quadros, M.L.E.S., 2006. Mapa Geológico do Estado do Amazonas, Escala 1:100.000. Ministério de Minas e Energia, Governo do estado do Amazonas. Serviço Geológico do Brasil (CPRM). Web site: www.cprm.gov.br (last accessed on 05/09/2014).
Figueiredo, J., Hoorn, C., van der Ven, P., Soares, E., 2009. Late Miocene onset of the Amazon River and the Amazon deep-sea fan: evidence from the Foz do Amazonas Basin. Geology 37, 619–622.
Filizola, N.P., 1999. O fluxo de sedimentos em suspensão nos rios da bacia Amazônica Brasileira. ANEEL, Brasilia (63 pp).
Fitzsimmons, K.E., 2011. An assesment of the luminescence sensitivity of Australian quartz with respect to sediment history. Geochronometria 38, 199–208.
Galehouse, J.S., 1971. Point counting. In: Carver, R.E. (Ed.), Procedures in Sedimentary Petrology. Wiley-Interscience, New York, pp. 385–407.
Govin, A., Chiessi, C.M., Zabel, M., Sawakuchi, A.O., Heslop, D., Hörner, T., Zhang, Y., Mulitza, S., 2014. Terrigenous input off northern South America driven by changes in Amazonian climate and the North Brazil Current retroflection during the last 250 ka. Climate of the Past Discussions 9, 5855–5898.
Griffin, W.L., Belousova, E.A., Walters, S.G., O'Reilly, S.Y., 2006. Archaean and Proterozoic crustal evolution in the Eastern Succession of the Mt Isa district, Australia: U–Pb and Hf-isotope studies of detrital zircons. Australian Journal of Earth Sciences 53, 125–149.
Grimm, A.M., 2011. Interannual climate variability in South America: impacts on seasonal precipitation, extreme events, and possible effects of climate change. Stochastic Environmental Research and Risk Assessment 25, 537–554.
Guedes, C.C.F., Giannini, P.C.F., Nascimento Jr., D.R., Sawakuchi, A.O., Tanaka, A.P.B., Rossi, M.G., 2011. Controls of heavy minerals and grain size in a holocene regressive barrier (Ilha Comprida, southeastern Brazil). Journal of South American Earth Sciences 31, 110–123.
Guyot, J.L., Jouanneau, J.M., Wasson, J.G., 1999. Characterisation of river bed and suspended sediments in the Rio Madeira drainage basin (Bolivian Amazonia). Journal of South American Earth Sciences 12, 401–410.
Guyot, J.L., Jouanneau, J.M., Soares, L., Boaventura, G.R., Maillet, N., Lagane, C., 2007. Clay mineral composition of river sediments in the Amazon Basin. Catena 71, 340–356.
Hayakawa, H.E., Rossetti, D.F., Valeriano, M.M., 2010. Applying DEM-SRTM for reconstructing paleodrainage in Amazonia. Earth and Planetary Science Letters 297, 262–270.
Hoorn, C., 1994. An environmental reconstruction of the palaeo-Amazon River system (Middle–Late Miocene, NW Amazonia). Palaeogeography, Palaeoclimatology, Palaeoecology 112, 187–238.
Hoorn, C., Guerrero, J., Sarmiento, G.A., Lorente, M.A., 1995. Andean tectonics as a cause for changing drainage patterns in Miocene, northern South America. Geology 23, 237–240.
Howard, K.E., Hand, M., Barovich, K.M., Reid, A., Wade, B.P., Belousova, E.A., 2009. Detrital zircon ages: improving interpretation via Nd and Hf isotopic data. Chemical Geology 262, 277–292.
Hubert, J.F., 1962. A zircon–tourmaline–rutile maturity index and the dependence of the composition of heavy mineral assemblages with the gross composition and texture of sandstones. Journal of Sedimentary Petrology 32, 440–450.
Instituto Geológico Minero y Metalurgico — INGEMMET, 1995. Mapa Geológico del Perú Escala 1:1.000.000 (digital version).
Koul, D.K., Chougaonkar, M.P., 2007. The pre-dose phenomenon in the OSL signal of quartz. Radiation Measurements 42, 1265–1272.
Latrubesse, E.M., Franzinelli, E., 2005. The late Quaternary evolution of the Negro river, Amazon, Brazil: implications for island and floodplain in large anabranching tropical systems. Geomorphology 70, 372–397.
Latrubesse, E.M., Stevaux, J.C., Sinha, R., 2005. Tropical rivers. Geomorphology 70, 187–206.
Li, S.H., 2002. Luminescence sensitivity changes of quartz by bleaching, annealing and UV exposure. Radiation Effects and Defects in Solids 157, 357–364.
Longo, R., Baldock, J., 1982. National Geologic Map of the Republic of Ecuador 1:1.000.000. Dirección General de Geología y Minas de Ecuador.
Lü, T., Sun, J., Li, S.-H., Gong, Z., Xue, L., 2014. Vertical variations of luminescence sensitivity of quartz grains from loess/paleosol of Luochuan section in the central Chinese Loess Plateau since the last interglacial. Quaternary Geochronology 22, 107–115.
Mange, M.A., Maurer, H.F.W., 1991. Heavy Minerals in Colour. Chapman & Hall, London.
Mange, M.A., Morton, A.C., 2007. Geochemistry of heavy minerals. In: Mange, M.A., Wright, D.T. (Eds.), Heavy Minerals in Use. Developments in Sedimentology 58, pp. 345–391.
Mange-Rajetzky, M.A., 1981. Detrital blue sodic amphibole in recent sediments, southern coast, Turkey. Journal of the Geological Society, London 138, 83–92.
Mangiarotti, S., Martinez, J.M., Bonnet, M.P., Buarque, D.C., Filizola, N., Mazzega, P., 2013. Discharge and suspended sediment flux estimated along the mainstream of the Amazon and the Madeira rivers (from in situ and MODIS Satellite Data). Journal of Applied Earth Observation and Geoinformation 21, 341–355.
Marsaglia, K.M., DeVaughn, A.M., James, D.E., Marden, M., 2010. Provenance of fluvial terrace sediments within the Waipaoa sedimentary system and their importance to New Zealand source-to-sink studies. Marine Geology 270, 84–93.
Martinelli, L.A., Forsberg, B.R., Victoria, R.L., Devol, A.H., Mortatti, J.R., Ferreira, J., Bonassi, J., de Oliveira, E., 1993. Suspended sediment load in the Madeira river. Mitteilungen aus dem Geologisch-Palaontologischen Institut der Universitat Hamburg 74, 41–54.
McKeever, S.W.S., Bøtter-Jensen, L., Agersnap Larsen, N., Mejdah, V., Poolton, N.R.J., 1996. Optically stimulated luminescence sensitivity changes in quartz due to repeated use in single aliquot readout: experiments and computer simulations. Radiation Protection Dosimetry 65, 49–54.
Meade, R.H., 1994. Suspended sediments of the modern Amazon and Orinoco rivers. Quaternary International 21, 29–39.
Meade, R.H., Dunne, T., Richey, J.E., De, M., Santos, U., Salati, E., 1985. Storage and remobilization of suspended sediment in the lower Amazon River of Brazil. Science 228, 488–490.

Meinhold, G., 2010. Rutile and its applications in earth sciences. Earth-Science Reviews 102, 1–28.
Monsch, K.A., 1998. Miocene fish faunas from the northwestern Amazonian basin (Colombia, Peru, Brazil) with evidence of marine incursions. Palaeogeography, Palaeoclimatology, Palaeoecology 143, 31–50.
Morton, A.C., Hallsworth, C.R., 1994. Identifying provenance-specific features of detrital heavy mineral assemblages in sandstones. Sedimentary Geology 90, 241–256.
Morton, A.C., Hallsworth, C.R., 1999. Processes controlling the composition of heavy mineral assemblages in sandstones. Sedimentary Geology 124, 3–29.
Morton, A.C., Humphreys, B., Dharmayanti, D.A., Sundoro, 1994. Palaeogeographic implications of the heavy mineral distribution in Miocene sandstones of the North Sumatra Basin. Journal of Southeast Asian Earth Sciences 10, 177–190.
Moska, P., Murray, A.S., 2006. Stability of the quartz fast-component in insensitive samples. Radiation Measurements 41, 878–885.
Nascimento, M.S., Góes, A.M., Macambira, M.B., Brod, J.A., 2007. Provenance of Albian sandstones in the São Luís Grajaú Basin (northern Brazil) from evidence of Pb–Pb zircon ages, mineral chemistry of tourmaline and palaeocurrent data. Sedimentary Geology 201, 21–47.
Oca, I.M., 1997. Geografía y recursos naturales de Bolivia. Edobol ed. (614 pp).
Pérez, H., Oller, V.J., Pareja, L., Trulfio, D.B., Araulbar, O.R., López, O., Fernandez, P.S., Ramirez, R.V.F., Ballón, A.R., Ramos, W.C., Llanos, A., 1996. Mapa Geológico de Bolívia, 1:1.000.000. Servício Nacional de Geología y Minería — SERGEOMIN/Yacimientos Petrolíferos Fiscales Bolivianos — YPFB.
Pettijohn, F.J., 1975. Sedimentary Rocks. Harper & Row Publs. Inc., New York, New York.
Pettijohn, F.J., Potter, P.E., Siever, R., 1972. Sand and Sandstone. Springer-Verlag Inc., New York.
Pietsch, T.J., Olley, J.M., Nanson, G.C., 2008. Fluvial transport as a natural luminescence sensitiser of quartz. Quaternary Geochronology 3, 365–376.
Reis, N.J., Almeida, M.E., Riker, S.L., Ferreira, A.L., 2006. Mapa Geológico do Estado do Amazonas, Escala 1:1.000.000. In: Relatório de Geologia e Recursos Minerais do Estado do Amazonas. Minist. De Minas e Energia, Convênio CPRM/CIAMA-AM, Manaus (AM), 153 pp.
Rhodes, E.J., 2011. Optically stimulated luminescence dating of sediments over the past 200,000 years. Annual Review of Earth and Planetary Sciences 39, 461–488.
Roche, M.A., Fernandez, C., 1988. Water resources, salinity and salt yields of the rivers of the Bolivian Amazon. Journal of Hydrology 101, 305–331.
Rossetti, D.F., Netto, R.G., 2006. First evidence of marine influence in the cretaceous of the Amazonas Basin, Brazil. Cretaceous Research 27, 513–528.
Sacek, V., 2014. Drainage reversal of the Amazon River due to the coupling of surface and lithospheric processes. Earth and Planetary Science Letters 401, 301–312.
Salinas, W.A., Vela, C., Davidson, J., Aceñolaza, F.G., 1989. Mapa Geológico de la América del Sur — Área Pacífica, 1:5.000.000.
Sawakuchi, A.O., Blair, M., DeWitt, R., Faleiros, F.M., Hyppolito, T.N., Guedes, C.C.F., 2011. Thermal history versus sedimentary history: OSL sensitivity of single quartz grains extracted from igneous and metamorphic rocks and sediments. Quaternary Geochronology 6, 261–272.
Sawakuchi, A.O., Guedes, C.C.F., DeWitt, R., Giannini, P.C.F., Blair, M.W., Nascimento Jr., D.R., Faleiros, F.M., 2012. Quartz OSL sensitivity as a proxy for storm activity on the southern Brazilian coast during the Late Holocene. Quaternary Geochronology 13, 92–102.
Schobbenhaus, C., Bellizia, A., 2001. Geological Map of South America, 1:5.000.000. CGMW – CPRM – DNPM – UNESCO, Brasília (cd-rom).
Sevastjanova, I., Hall, R., Alderton, D., 2012. A detrital heavy mineral viewpoint on sediment provenance and tropical weathering in SE Asia. Sedimentary Geology 280, 179–194.
Shephard, G.E., Müller, R.D., Liu, L., Gurnis, M., 2010. Miocene drainage reversal of the Amazon River driven by plate–mantle interaction. Nature Geoscience 3, 870–875.
Silva, M.S.R., Cunha, H.B., Miranda, S.A.F., Abrantes, N.G., Santana, G.P., 2010. Rios da Amazônia: uma contribuição para a classificação de acordo com seus usos preponderantes. Anais da Sociedade Brasileira de Pesquisa Científica 210 (ISSN 2178-3969), 1287.
Silva, C.R., Peixinho, F.C., Monteiro, A., Pinto, E.J.A., Azambuja, A.M.S., Farias, J.A.M., Pickbrenner, K., Weschendelder, A.B., Santos, A.L.M.R., Marcuzzo, F.F.N., Costa, M.R., Nascimento, J.R.S., Furtunato, O.M., Medeiros, V.S., Almeida, I.S., 2011. Levantamento da geodiversidade. Projeto Atlas Pluviométrico do Brasil – isoietas anuais médias, período 1977 a 2006. CPRM, escala 1:1.000.000.
Siqueira, L.P., 1989. Bacia do Parecis. Boletim de Geociências da Petrobrás 3, 3–16.
Slingerland, R., Smith, N.D., 2004. River avulsions and their deposits. Annual Review of Earth and Planetary Sciences 32, 257–285.
Soares, E.A.A., Tatumi, S.H., Riccomini, C., 2010. OSL age determinations of Pleistocene fluvial deposits in Central Amazonia. Anais da Academia Brasileira de Ciências 82, 691–699.
Stouthamer, E., Berendsen, H.J.A., 2001. Avulsion frequency, avulsion duration and interavulsion period of Holocene channel belts in the Rhine-Meuse delta, The Netherlands. Journal of Sedimentary Research B71, 558–597.
Stouthamer, E., Berendsen, H.J.A., 2007. Avulsion: the relative roles of autogenic and allogenic processes. Sedimentary Geology 198, 309–325.
Tanaka, A.P.B., Giannini, P.C.F., Fornari, M., Nascimento Jr., D.R., Sawakuchi, A.O., Rodrigues, S.I., Menezes, P.M.L., DeBlasis, P., Porsani, J.L., 2009. A planície costeira holocênica de Campos Verdes (Laguna, SC): evolução sedimentar inferida a partir de georradar (GPR), granulometria e minerais pesados. Revista Brasileira de Geociencias 39, 751–767.
Tapias, J.G., Guevara, A.N., Ramírez, N.E.M., Mejía, D.M.J., Avella, M.L.T., Ospina, J.S., Naranjo, J.A.O., Narváez, T.G., Diederix, H., Peña, H.U., Penagos, M.M., 2007. Mapa Geológico de Colombia 1:2.800.000, Instituto Colombiano de Geología y Minería.
Tassinari, C.C.G., Macambira, M.J.B., 2000. Geochronological provinces of the Amazonian Craton. Episodes 22, 174–182.
Triebold, S., von Eynatten, H., Luvizotto, G.L., Zack, T., 2007. Deducing source rock lithology from detrital rutile geochemistry: an example from the Erzgebirge, Germany. Chemical Geology 244, 421–436.
Van Andel, T.H., 1958. A defense of the term alterite. Journal of Sedimentary Petrology 28, 234–235.
Vera, C., Higgins, W., Amador, J., 2006. Towards a unified view of the American Monsoon Systems. Journal of Climate 19, 4977–5000.
Viers, J., Roddaz, M., Filizola, N., Guyot, J.-L., Sondag, F., Brunet, P., Zouiten, C., Boycayrand, C., Martin, F., Boaventura, G.R., 2008. Seasonal and provenance controls on Nd–Sr isotopic compositions of Amazon rivers supended sediments and implications for Nd and Sr fluxes exported to the Atlantic Ocean. Earth and Planetary Science Letters 274, 511–523.
Vital, H., Stattegger, K., Garbe-Schonberg, C.-D., 1999. Composition and trace-element geochemistry of detrital clay and heavy-mineral suites of the lowermost Amazon river: a provenance study. Journal of Sedimentary Research 69, 563–575.
Wesslingh, F.P., Räsänen, M.E., Irion, G., Vonhof, H.B., Kaandorp, R., Renema, W., Romero-Pittman, L., Gingras, M., 2001. Lake Pebas: a palaeoecological reconstruction of a Miocene long-lived lake complex in western Amazonia. Cainozoic Research 1, 35–81.
Wolinsky, M.A., Swenson, J.B., Paola, C., Voller, V.R., 2010. Source to Sink sediment dynamics: making models talk to data. AGU Chapman Conference — Source to Sink Systems Around the World and Through Time (Oxnard, CA, Abstracts, 77 pp).
Zack, T., von Eynatten, H., Kronz, A., 2004. Rutile geochemistry and its potential use in quantitative provenance studies. Sedimentary Geology 171, 37–58.